Low-Temperature Magnetic Properties of Some Hexagonal Rare-Earth Trihalides

J. H. COLWELL, B. W. MANGUM, AND D. B. UTTON*
National Bureau of Standards, Washington, D. C. 20234
(Received 2 December 1968)

We have made measurements of the low-temperature heat capacity, magnetic susceptibility, and chlorine nuclear quadrupole resonance (NQR) of $CeCl_3$, $PrCl_3$, $NdCl_3$, $SmCl_3$, and $CeBr_3$. Some measurements have been made on $PrBr_3$ and $NdBr_3$. The experimental results can be closely correlated with antiferromagnetic linear chain models. The NQR shows that long-range order occurs in $PrCl_3$ at 0.428 K. In $NdCl_3$, the NQR line disappeared at 0.50 K and the resonances produced by an internal field appeared at 0.17 K. In $CeCl_3$, the NQR resonance disappeared at 0.110 K and no lines were found above 0.054 K. In $SmCl_3$, the NQR line disappeared at 0.21 K and no resonance was observed above 0.1 K. We have measured the internal field, which is proportional to the sublattice magnetization, at the chlorine nucleus in $PrCl_3$ and $NdCl_3$ below their Néel temperatures, and have determined the magnitude and the direction of the internal field at the chlorine nucleus relative to the principal axes of the electric field gradient.

1. INTRODUCTION

IN the past few years there has been considerable interest in the rare-earth trihalides, both concentrated and dilute, and their magnetic properties have been investigated by a variety of techniques. Of all the rare-earth compounds, the hexagonal trihalides are probably the most attractive for study. They have a simple crystal structure[1,2] containing only two simple ionic species and all the rare-earth ions are magnetically equivalent. Also, because the lanthanum trihalides are members of this series, magnetically dilute crystals can be grown which permit measurements which would not otherwise be possible.

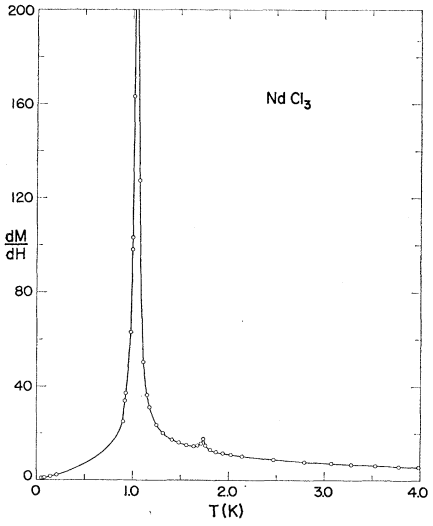

FIG. 1. Temperature dependence of the differential susceptibility, in arbitrary units, of the 5N's $NdCl_3$ sample with the ac measuring field parallel to the c axis of the crystal. The susceptibility reaches a maximum value of 321 at 1.04 K.

In spite of their attractiveness there is a paucity of experimental data on the concentrated rare-earth trihalides. This is due in part to the difficulty of preparing large, pure crystals. The only one of these compounds which can be considered well characterized is $GdCl_3$. Magnetic susceptibility[3] and heat capacity[4] measurements show this compound to order ferromagnetically with a Curie temperature of 2.2 K. Eisenstein, Hudson, and Mangum[5] measured the susceptibilities of

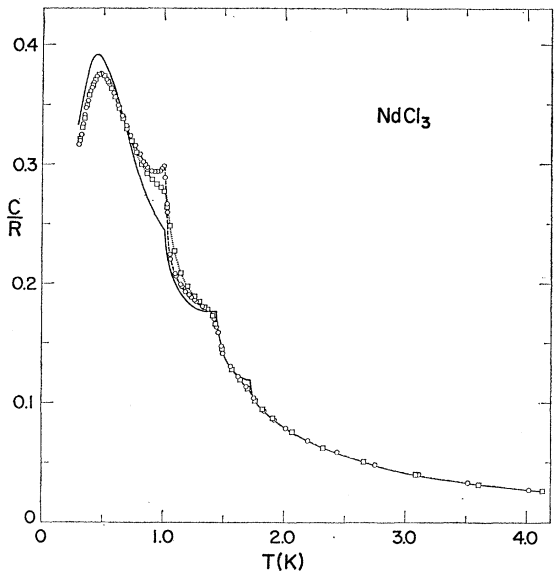

FIG. 2. Heat capacity of $NdCl_3$. The open circles represent the heat capacity of the 5N's $NdCl_3$ sample in zero field and the squares represent measurements made in a magnetic field of approximately 5×10^{-2} T applied parallel to the c axis of the crystal. The solid line represents the heat capacity of the 3N's $NdCl_3$ sample (Ref. 31).

* Presently at Materials Physics Division, Atomic Energy Research Establishment Harwell, Didcot, Berkshire, United Kingdom.

[1] W. H. Zachariasen, J. Chem. Phys. **16**, 254 (1948).

[2] D. H. Templeton and C. H. Dauben, J. Am. Chem. Soc. **76**, 5237 (1954).

[3] W. P. Wolf, M. J. M. Leask, B. W. Mangum, and A. F. G. Wyatt, J. Phys. Soc. Japan Suppl. B-1, **17**, 487 (1961).

[4] M. J. M. Leask, W. P. Wolf, and A. F. G. Wyatt, in *Proceedings of The Eighth International Conference on Low Temperatures, London, September 1962* (Butterworths Scientific Publications Ltd., Washington, D. C., 1963), p. 230.

[5] J. C. Eisenstein, R. P. Hudson, and B. W. Mangum, Phys. Rev. **137**, A1886 (1965).

the other trichlorides of the series, $CeCl_3$, $PrCl_3$, $NdCl_3$, and $SmCl_3$, and found each of them to indicate antiferromagnetic behavior at low temperatures. $CeCl_3$ and $NdCl_3$ exhibited sharp spikes in the susceptibility which were interpreted as cooperative magnetic transitions. Keen, Landau, and Wolf[6] have made a brief report of magnetic susceptibility and heat capacity measurements on $CeCl_3$. Prinz[7] has been able to measure the optical spectra of pure $NdCl_3$ and $NdBr_3$ and observe effects due to interactions between the magnetic ions.

By comparison there is a large amount of experimental data on the magnetically dilute crystals. Hutchison and Wong[8] have carried out an electron spin resonance (ESR) study of the various rare-earth ions diluted in $LaCl_3$. Dieke and others[9–22] have made extensive studies of the optical spectra of the rare-earth trihalides. Those measurements yield g values, values of the crystal field splittings, and nuclear hyperfine interactions which can be carried over to the study of the concentrated crystals. Of importance in elucidating the nature of the low-temperature magnetic ordering in the concentrated crystals are the ESR determinations of interactions between ions in isolated pairs in dilute crystals.[23–30]

Here we report measurements on several rare-earth trihalide crystals which were conducted in an effort to determine the type and extent of magnetic ordering occurring in these materials at low temperatures. We have measured the heat capacities of four of the crystals used in the susceptibility measurements of Eisenstein *et al.*[5] Magnetic susceptibilities and heat capacities of new crystals of $PrCl_3$ and $NdCl_3$ have been measured. The temperature dependence of the ^{35}Cl nuclear quadrupole resonances (NQR) in $CeCl_3$, $PrCl_3$, $NdCl_3$, and $SmCl_3$ crystals (and ^{37}Cl in $NdCl_3$) were studied in order to determine if long-range order occurs and at what temperatures. Measurements have also been made on $CeBr_3$, $PrBr_3$, and $NdBr_3$. Heat capacities of $PrCl_3$ and $NdCl_3$ have been reported previously[31] as well as some preliminary ^{35}Cl NQR results.[32]

2. EXPERIMENTAL

A. Crystal Preparation

The crystals were prepared by a method due to Wong.[33] The hydrated trichloride or tribromide is prepared in a straightforward manner from commercially available 99.9%-pure oxide. It is then dehydrated by warming slowly to its melting point under vacuum. Single crystals are grown from the polycrystalline material in quartz tubes containing helium gas at 3×10^4 N m^{-2} (1 N m^{-2} = 0.0075 Torr) by slowly lowering the tubes through a furnace which is maintained at a constant temperature. All handling of unprotected crystals was done in a dry box.

Crystals of $PrCl_3$ and $NdCl_3$ were also prepared from 99.999%-pure oxides. These two crystals are labeled 5N's to distinguish them from the others, which we label 3N's.

B. Susceptibility Measurements

The differential magnetic susceptibilities were measured with an ac mutual induction bridge apparatus.[5] Temperatures below 1 K were obtained by the adiabatic demagnetization method. The refrigerator salt, either chromic potassium alum or manganous ammonium sulfate, was used not only as refrigerant but also as the thermometer. The thermal link connecting cooling salt to sample consisted of several hundred fine copper wires "potted" in the salt with epoxy. Their free ends were tied on to the sample with thread and covered liberally with stopcock grease. Separate coil systems surrounding salt and sample were external to a glass vacuum case in the liquid-helium bath.

C. Heat Capacity Measurements

For the heat capacity measurements the hygroscopic rare-earth trihalide samples were encapsulated in a thin-walled copper calorimeter vessel. A small amount of ^3He was sealed in the vessel to ensure thermal contact. The

[6] B. E. Keen, D. P. Landau, and W. P. Wolf, Bull. Am. Phys. Soc. **11**, 377 (1966).
[7] G. A. Prinz, Phys. Letters **20**, 323 (1966); Phys. Rev. **152**, 474 (1966).
[8] C. A. Hutchison, Jr., and E. Wong, J. Chem. Phys. **29**, 754 (1958).
[9] G. H. Dieke and R. Sarup, J. Chem. Phys. **29**, 741 (1958).
[10] E. V. Sayre, K. M. Sancier, and S. Freed, J. Chem. Phys. **23**, 2060 (1955); **29**, 242 (1958).
[11] B. Schneider, Z. Physik **177**, 179 (1964).
[12] E. Carlson and G. H. Dieke, J. Chem. Phys. **29**, 229 (1958).
[13] E. H. Carlson and G. H. Dieke, J. Chem. Phys. **34**, 1602 (1961).
[14] F. Varsanyi and G. H. Dieke, J. Chem. Phys. **33**, 1616 (1960).
[15] M. S. Magno and G. H. Dieke, J. Chem. Phys. **37**, 2354 (1962).
[16] F. Varsanyi and G. H. Dieke, J. Chem. Phys. **36**, 835 (1962).
[17] L. G. DeShazer and G. H. Dieke, J. Chem. Phys. **38**, 2190 (1963).
[18] E. V. Sayre and S. Freed, J. Chem. Phys. **24**, 1211 (1956).
[19] K. S. Thomas, S. Singh, and G. H. Dieke, J. Chem. Phys. **38**, 2180 (1963).
[20] H. M. Crosswhite and G. H. Dieke, J. Chem. Phys. **35**, 1535 (1961).
[21] G. H. Dieke and S. Singh, J. Chem. Phys. **35**, 555 (1961).
[22] J. T. Hougen and S. Singh, Proc. Roy. Soc. (London) **A277**, 193 (1964).
[23] M. T. Hutchings and W. P. Wolf, in *Proceedings of The International Conference on Magnetism, Nottingham, 1964* (Institute of Physics and the Physical Society, London, 1964), p. 342.
[24] R. J. Birgeneau, M. T. Hutchings, and R. N. Rogers, Phys. Rev. Letters **16**, 584 (1966).
[25] K. L. Brower, H. J. Stapleton, and E. O. Brower, Phys. Rev. **146**, 233 (1966).
[26] J. M. Baker, J. D. Riley, and R. G. Shore, Phys. Rev. **150**, 198 (1966).
[27] J. M. Baker, R. J. Birgeneau, M. T. Hutchings, and J. D. Riley, Phys. Rev. Letters **21**, 620 (1968).
[28] R. J. Birgeneau, M. T. Hutchings, and W. P. Wolf, J. Appl. Phys. **38**, 957 (1967).
[29] D. P. Landau, R. J. Birgeneau, M. T. Hutchings, and W. P. Wolf, J. Appl. Phys. **39**, 975 (1968).
[30] M. T. Hutchings, R. J. Birgeneau, and W. P. Wolf, Phys. Rev. **168**, 1026 (1968).
[31] J. H. Colwell and B. W. Mangum, J. Appl. Phys. **38**, 1468 (1967).
[32] B. W. Mangum and D. B. Utton, Bull. Am. Phys. Soc. **12**, 1043 (1967).
[33] E. Y. Wong (private communication).

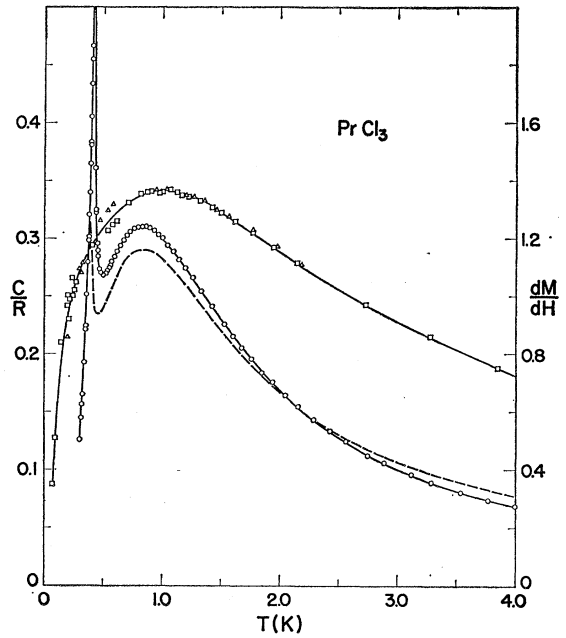

FIG. 3. Differential magnetic susceptibility and heat capacity of the 5N's $PrCl_3$ sample. The triangles and squares represent two separate susceptibility determinations expressed in arbitrary units with the results normalized at 1 K. The circles represent the heat capacity measurements. The heat capacity reaches a maximum of $0.60R$ at 0.41 K. The dashed curve represents the heat capacity of the 3N's sample (Ref. 31).

thermometer and heater were mounted on the outside of the vessel. The calorimeter vessel was suspended by nylon threads in the inner vacuum jacket of a ^{3}He refrigerator. A mechanical heat switch, making contact between the refrigerator and the calorimeter vessel, was used to cool and subsequently isolate the vessel. The heat capacity measurements were made by the usual discontinuous heating method.

The germanium resistance thermometer used in these measurements was calibrated against the ^{3}He and ^{4}He vapor pressure scales.[34,35] The calibration points between 0.3 and 4.2 K were fitted to well within the experimental error by the expression

$$\log_{10}R=\sum_{i=0}^{n}A_i(\log_{10}T)^i,$$

with $n=4$. As a check on the temperature scale and also on the calorimetric measurements, the heat capacity of a standard copper sample[36] was measured. The measured heat capacity, compared with the expression $C/R=\gamma T+AT^3$ with γ and A having the values given in Ref. 36, was approximately $\frac{1}{2}\%$ low at 0.3 K, $\frac{1}{2}\%$ high at 1 K, and 1% low at 4 K.

[34] R. H. Sherman, S. G. Sydoriak, and T. R. Roberts, J. Res. Natl. Bur. Std. (U.S.) **68A**, 579 (1964).
[35] F. G. Brickwedde, H. Van Dijk, M. Durieux, J. R. Clement, and J. K. Logan, Natl. Bur. Std. (U.S.) Monograph **10** (1960).
[36] D. W. Osborne, H. E. Flotow, and F. Schreiner, Rev. Sci. Instr. **38**, 159 (1967).

The ^{3}He exchange gas used for thermal contact inside the calorimeter vessel is a potential source of error in these measurements. It was found that ^{3}He is strongly adsorbed on the rare-earth trihalide crystals. With the $PrCl_3$ and $NdCl_3$ samples and 10^2 N m^{-2} of ^{3}He gas sealed in the vessel at room temperature, thermal contact between sample and vessel was lost at 1 K. Approximately 10^3 N m^{-2}, the amount used in the measurements reported here, was required to maintain good thermal contact to 0.3 K. The heat capacity of $PrCl_3$ has been measured with 5×10^3 N m^{-2} of ^{3}He gas in the vessel (see Fig. 2 of Ref. 31) and found to differ from measurements with 10^3 N m^{-2} only above 2.5 K, where it was 1–2% greater. $SmCl_3$ has also been measured with two different amounts of exchange gas and no difference observed in the results (see Sec. 3 D). We assume that 10^3 N m^{-2} of ^{3}He exchange gas has little or no effect on the measured heat capacity.

The data were corrected for the heat capacity of the calorimeter vessel, thermometer, etc., which was determined in a separate experiment, but no other corrections were applied. The overall uncertainty in the sample heat capacity is estimated to be less than 1% below 2 K but may be as large as 5% at 4 K.

D. NQR Measurements

The NQR of ^{35}Cl and ^{37}Cl were first observed with a super-regenerative oscillator and Zeeman modulation at 77 K. All measurements at 4.2 K and below were made with a high-level Robinson oscillator[37] frequency-modulated at 40 Hz with phase-sensitive detection at 80 Hz.

Temperatures down to 0.13 K were achieved in an adiabatic demagnetization arrangement nearly identical with that used in the susceptibility measurements. In a typical experiment the refrigerant and specimen achieved thermal equilibrium, as indicated by the temperature drift rate, 30 min after demagnetization. In some cases the thermometry could be checked by observation of the NQR signal intensity which is proportional to the Boltzmann factor.

In one experiment a ^{3}He-^{4}He dilution refrigerator was used to cool a $CeCl_3$ sample. A spherical single crystal of cerous magnesium nitrate (CMN) was used as a thermometer. The sample was suspended approximately 5 cm below the dilution chamber and the CMN was suspended approximately 5 cm below that. An oscillator level of 50 mV resulted in rf heating of 0.4–0.5 μW. During the experiment the oscillator level was sufficiently low such that the rf heating was negligible; we were unable to detect any change in temperature when the oscillator was switched either on or off. In both this and the adiabatic demagnetization experiments the sample coil was wound on a glass envelope which surrounded the sample and thermometer; hence, the coil remained at the temperature of the pumped helium

[37] D. T. Edmonds and F. N. H. Robinson, J. Sci. Instr. **44**, 475 (1967).

bath. This arrangement resulted in a filling factor of approximately 20%. Coaxial stainless-steel tubes, 120 cm in length, connected the sample coil with the oscillator.

3. RESULTS

A. $NdCl_3$

The differential susceptibility of the 3N's $NdCl_3$ sample, which has been described in great detail,[5] is characterized by two sharp spikes of approximately equal height appearing at 1.04 and 1.74 K. In the susceptibility of the 5N's sample shown in Fig. 1 the relative sizes of the peaks are considerably different. The peak at 1.04 K is more than three times higher than that found in the 3N's sample, while the peak at 1.74 K is smaller by a factor of 20. Above 2.5 K the susceptibilities of the two samples are the same and obey the Curie law.

The heat capacity of $NdCl_3$, as represented by the 3N's and 5N's samples shown in Fig. 2, has a broad anomaly with a maximum at approximately 0.47 K. Small peaks appear in the heat capacity at the temperatures of the spikes in the magnetic susceptibility and there appears to be a close correlation between their size and the size of the corresponding susceptibility spikes. A third small peak appears in the heat capacity at 1.45 K, a temperature where the magnetic susceptibility is nearly constant.

Application of a magnetic field causes a pronounced broadening of the 1.04-K heat capacity peak but no discernible effects at other temperatures. Of course, the 1.74-K peak in the 5N's sample is so small that no field effect could be detected.

The ^{35}Cl NQR frequency in $NdCl_3$ is 4.729 MHz at 4.2 K and the linewidth is 11.6 kHz. No resonances could be observed in the temperature range $0.17<T<0.50$ K. Below 0.17 K, lines were observed at 6.73, 5.26, and 4.67 MHz with linewidths of 15 ± 2 kHz and the relative intensities were 1.5:10:1, respectively. Weak resonances due to ^{37}Cl were detected at 3.82 and 4.26 MHz. No other resonances were found in the range 3.16–9.10 MHz. No change in NQR frequencies was observed in the range 0.5–4.2 K. At 1.04 and 1.74 K, however, the sample became lossy, as was observed in the susceptibility measurements[5] at these temperatures.

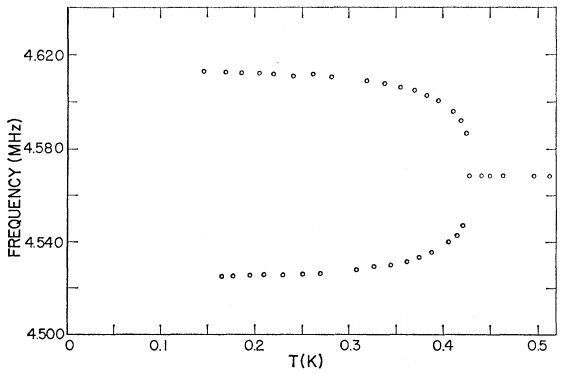

FIG. 4. Temperature dependence of the NQR frequencies in $PrCl_3$.

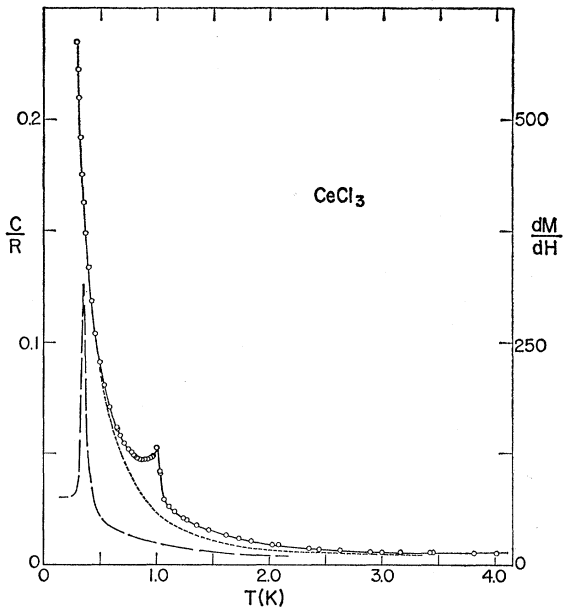

FIG. 5. Heat capacity and magnetic susceptibility of $CeCl_3$. The open circles are the heat capacity data points. The long-dashed curve represents the susceptibility with the measuring field parallel to the c axis of the crystal (Ref. 5). The short-dashed curve is the linear Ising model given by $C/R=(0.155/T)^2\,\mathrm{sech}^2(0.155/T)$.

B. $PrCl_3$

Above 1 K the differential susceptibility of the 5N's $PrCl_3$ sample, which is shown in Fig. 3, is identical with that of the 3N's sample. Below 1 K, however, the susceptibility of the 3N's sample remained approximately constant down to about 0.4 K, below which it again increased slowly with decreasing temperature. The susceptibility of $PrCl_3$ is extremely small, so that the behavior of the 3N's sample below 1 K could easily result from a small amount of another magnetic rare-earth impurity.

The heat capacities of the 3N's and the 5N's $PrCl_3$ samples are compared in Fig. 3, where they are represented by the dashed-curve and the open-circle data points, respectively. Above 0.5 K the results are very similar, with both samples having a broad maximum at 0.85 K, but the magnitude of the heat capacity of the 5N's sample varies from 5% greater at 1 K to 5% smaller at 4 K. Below 0.5 K, however, their behavior is quite different. The heat capacity of the 5N's sample reaches a maximum of $0.60R$ at 0.41 K, while the maximum of the 3N's sample is $0.32R$ at 0.37 K. Below 0.37 K the heat capacities of the two samples are nearly identical. The heat capacity of the 5N's $PrCl_3$ sample in a magnetic field of 5×10^{-2} T applied parallel to the c axis did not differ from the zero-field measurements.

The ^{35}Cl NQR frequency in $PrCl_3$ is 4.5685 MHz at 4.2 K and the linewidth is 6.8 kHz. In the 5N's $PrCl_3$

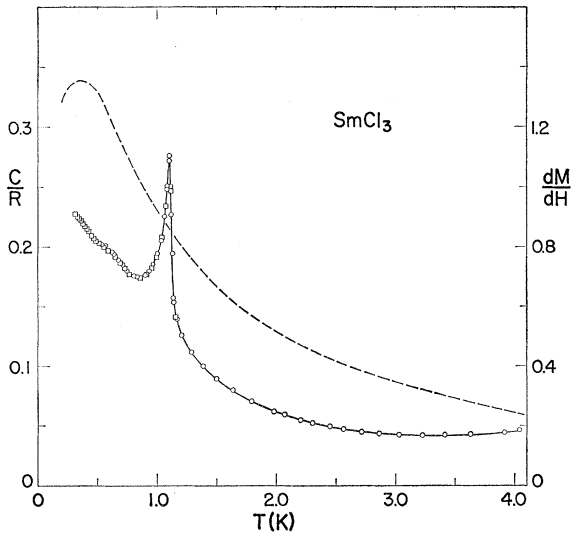

FIG. 6. Heat capacity and magnetic susceptibility of polycrystalline $SmCl_3$. The squares and circles are the heat capacity data points from two separate determinations. The dashed curve represents the magnetic susceptibility from Ref. 5.

sample the line splits into two components below 0.428 K in general agreement with the observations of Hessler and Carlson.[38] Figure 4 shows the observed nuclear resonance frequencies as a function of temperature. The shape of the lines changed progressively from the expected second derivative (but with unobserved inner wings) at the lowest temperature to sigmoid as the transition temperature was approached. A search was made for other lines below 0.428 K; nothing was found in the range 4.40–5.15 MHz. The signal-to-noise ratio for the observed lines at the lowest temperature was 10:1.

C. $CeCl_3$

The magnetic susceptibility of the $CeCl_3$ sample, which has been described earlier,[5] is represented in Fig. 5 by the long-dashed curve. The sharp spike in the susceptibility occurs at 0.345 K. The heat capacity, as given by the data points in the figure, shows no indication of a peak at 0.345 K, although it could possibly be obscured because of the steep slope of the heat capacity curve. Conversely, the susceptibility is varying smoothly at 1.0 K, where the small sharp peak occurs in the heat capacity. The heat capacity was not affected by a magnetic field of 5×10^{-2} T.

The ^{35}Cl NQR frequency in $CeCl_3$ is 4.387 MHz at 4.2 K and the linewidth is 9 kHz. The signal intensity was inversely proportional to temperature down to 0.20 K; below this temperature the intensity decreased without broadening and could no longer be observed below 0.110 K. The signal-to-noise ratio at 0.15 K was greater than 100:1. Unsuccessful searches were made for nuclear resonances in the frequency range 3.47–5.18 MHz at 0.054 K, the lowest temperature at which measurements were made, and also in the range 4.14–5.11 MHz at 0.080 K.

[38] J. P. Hessler and E. H. Carlson, J. Appl. Phys. **39**, 1014 (1968).

D. $SmCl_3$

The $SmCl_3$ sample used in these measurements was polycrystalline. The susceptibility, as reported earlier,[5] is represented by the dashed curve in Fig. 6 and the data points represent the heat capacity measurements. A pronounced thermal relaxation was observed in the heat capacity measurements below 1 K. This was originally thought to be due to poor thermal contact with the sample because of insufficient exchange gas in the calorimeter vessel. A second determination with 5×10^3 N m^{-2} of exchange gas gave the same result, indicating that the thermal resistance was in the sample itself. A field of 5×10^{-2} T had no effect on the measured heat capacity.

The ^{35}Cl NQR frequency in $SmCl_3$ is 5.033 MHz at 4.2 K with a linewidth of 12 kHz. The signal began to broaden and lose intensity at approximately 0.32 K and had disappeared at 0.21 K. No signal was found between 0.13 and 0.205 K in the frequency range 4.03–5.90 MHz.

E. $CeBr_3$

The g values for 0.25% Ce^{3+} in $LaBr_3$, measured by ESR,[39] were found to be $g_{\parallel}=4.044\pm0.007$ and $g_{\perp}\leq0.1$. The g values in the concentrated salt appear to have the same values as they have in the dilute salt.

The upper curve in Fig. 7 represents the magnetic susceptibility measured parallel to the c axis. The maximum susceptibility occurs at 0.25 K. We were unable to measure the susceptibility perpendicular to the c axis because of the small value of $g_{\perp}$. The sample was roughly the shape of a 2:1 ellipsoid and the Weiss

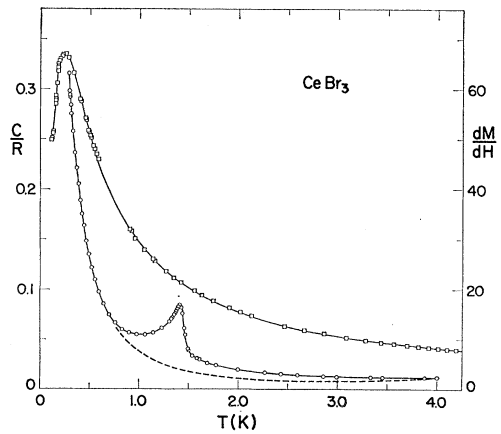

FIG. 7. Heat capacity and magnetic susceptibility of $CeBr_3$. The circles of the lower curve are the heat capacity data points. The squares of the upper curve are the susceptibility measurements made with the field parallel to the c axis of the crystal. The dashed curve is the linear Ising model given by $C/R=(0.196/T)^2\,\mathrm{sech}^2(0.196/T)$.

[39] R. P. Hudson and B. W. Mangum (unpublished).

constant determined from the high-temperature data is $\theta=+0.14$ K for $\chi=C/(T+\theta)$.

The heat capacity shown as the lower curve in Fig. 7 has a small peak at 1.42 K for which no indication is found in the susceptibility. The heat capacity was not affected by a magnetic field of 5×10^{-2} T.

We have observed the ^{81}Br and ^{79}Br NQR in $CeBr_3$ at 77 K using a super-regenerative oscillator. The ^{81}Br NQR line was found at 30.0 MHz and the ^{79}Br NQR line at 36.2 MHz.

F. $PrBr_3$

We have observed the ^{81}Br NQR at 31.0 MHz in $PrBr_3$ at 77 K using a super-regenerative oscillator.

G. $NdBr_3$

The g values of Nd^{3+} in $LaBr_3$ have been measured by Johnston and Wong[40] and are $g_{\parallel}=3.853$ and $g_{\perp}=1.903$. Prinz[7] gives $g_{\parallel}=3.8$ for pure $NdBr_3$. We have measured the magnetic susceptibility parallel to the c axis of $NdBr_3$ in the pumped ^{4}He region and it exhibits a broad maximum at 1.31 K.

We have observed the ^{81}Br and ^{79}Br NQR from one of the two nonequivalent bromine sites,[41] the "c" site, in $NdBr_3$ at 77 K using a super-regenerative oscillator. The ^{81}Br NQR line was found at 45.5 MHz and the ^{79}Br NQR line at 55.0 MHz. Parks and Moulton[42] have observed and reported the resonances for both bromine sites and find that the bromine NQR signal disappears at 4.2 K and, in agreement with their results, we were unable to find the bromine NQR signal at 4.2 K.

4. DISCUSSION

The crystal structure of the rare-earth trichlorides in the series $LaCl_3$ through $GdCl_3$ is hexagonal with two molecules per unit cell. The space group[1] is $C6_3/m(C_{6h}^2)$ and the point symmetry at the rare-earth site is C_{3h}. The rare-earth ions are all magnetically equivalent. A section of this structure is shown in Fig. 8, where the small spheres represent the rare-earth ions and the large spheres the chloride ions. Each rare-earth ion is surrounded by nine chloride ions, all very nearly the same distance from the rare-earth ion. Three are coplanar with the rare-earth ion and perpendicular to the c axis, and the other six lie three in a parallel plane above and three in a parallel plane below the rare-earth ion. Each rare-earth ion has two nearest-neighbor rare-earth ions which lie along the symmetry axis and six next-nearest neighbors only slightly farther away. The third-nearest rare-earth neighbors lie in planes perpendicular to the c axis at a distance nearly twice as large as that of the nearest neighbors.

The crystal structure[1] of $CeBr_3$ and $PrBr_3$ is the same as that of the corresponding trichloride. $NdBr_3$ has the layered orthorhombic structure of the $PuBr_3$ type,[41] and is therefore not a member of the principal series of compounds under consideration.

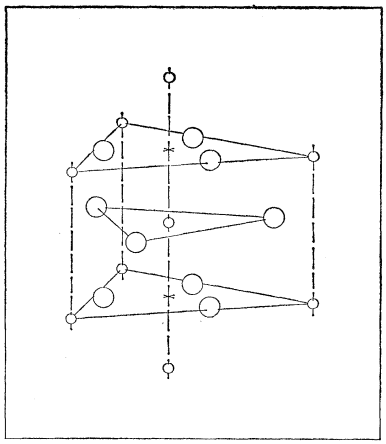

FIG. 8. Arrangements of the rare-earth and chloride ions in the hexagonal rare-earth trichloride crystals. The small spheres represent the rare-earth ions and the large spheres represent the chloride ions. The c axis is parallel to the dashed lines connecting the small spheres. The solid lines form planes perpendicular to the c axis.

For the three Kramers ions studied, Ce^{3+}, Nd^{3+}, and Sm^{3+}, the ground-state doublets in the trichlorides lie, respectively, 67.6, 166.0, and 58.6 K below the first excited state.[11,13,15] Pr^{3+} is not a Kramers ion; however, the point symmetry is such that an "accidental" ground-state doublet occurs with a splitting,[8] Δ, of $\sim$0.03 K. This level lies 47.6 K below the first excited state which is a singlet.[9,10] Values of these splittings in the tribromides are not available, but we assume that they are close to those of the trichlorides.[43] Below 4 K only the ground-state doublets are significantly populated, so we describe these systems by an effective spin $S=\frac{1}{2}$.

In the hexagonal trihalides the type of magnetic ordering occurring at low temperatures will be mainly determined by interactions between nearest-neighbor and next-nearest-neighbor rare-earth ions. Considerable information about these interactions is available from studies of the ESR pair spectra of Ce^{3+} and Nd^{3+} in $LaCl_3$ and $LaBr$,[24–27] and Gd^{3+} in $LaCl_3$ and $EuCl_3$.[28,30] In the gadolinium salt the nearest-neighbor interactions are antiferromagnetic and the next-nearest-neighbor interactions are ferromagnetic, with the latter being the larger. As a result, $GdCl_3$ orders ferromagnetically[3] at 2.2 K, a phenomenon which has been studied extensively. Ce^{3+} and Nd^{3+} in both the trichlorides and tribromides also have antiferromagnetic nearest-neighbor and ferromagnetic next-nearest-neighbor interactions but with the next-nearest-neighbor interactions being small compared with the nearest-neighbor interactions.

This has interesting consequences, since the domi-

[40] D. R. Johnston and E. Y. Wong, Bull. Am. Phys. Soc. **10**, 1201 (1965).
[41] W. H. Zachariasen, Acta Cryst. **1**, 265 (1948).
[42] S. I. Parks and W. G. Moulton, Phys. Letters **26A**, 63 (1967).
[43] I. Richman and E. Y. Wong, J. Chem. Phys. **37**, 2270 (1962).

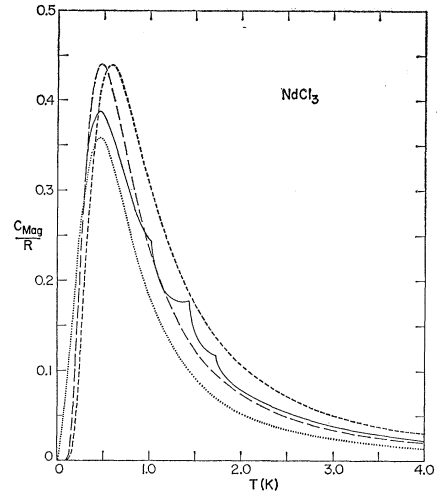

FIG. 9. Magnetic heat capacity of $NdCl_3$. The solid line is the experimental curve for the 3N's sample. The dashed lines are the linear Ising chain models with $J/k=-1.13$ and -1.32 K for the long and short dashes, respectively. The dotted curve is the linear chain model with intermediate anisotropy of $\gamma=0.5$ and $J/k=-0.72$ K.

nance of the nearest-neighbor interactions will result in the ions ordering in antiferromagnetic linear chains along the c axis. This by itself does not lead directly to a long-range-ordered structure and, in fact, appears to preclude any simple ordered structure. One can see from Fig. 8 that with ions antiferromagnetically aligned along the c axis the symmetrical arrangement of the next-nearest-neighbor ions about a given ion will cause their interactions with that ion to cancel.[31] Longer-range interactions, which are most probably dipolar, either cancel or tend to align the ions which lie in planes perpendicular to the c axis into what is equivalent to the highly degenerate antiferromagnetic triangular net arrangement.[29,44] Consequently, we may expect these compounds to behave as antiferromagnetic linear chains over a considerable range of temperature.

In the measured heat capacities there are lattice and nuclear hyperfine contributions which must be subtracted to obtain the "magnetic" heat capacity. The lattice heat capacity of the trichlorides is assumed to be the same as the measured value[45] in $LaCl_3$. This is only $0.004R$ at 4 K and varies as T^3. The lattice heat capacity of the tribromides was estimated to be twice as large as that of the trichlorides. Hyperfine contributions to the heat capacity were calculated from the expression given by Bleaney[46] using the parameters of Hutchison and Wong.[8] This contribution varies as T^{-2} and is just becoming significant in these compounds at 0.3 K.

A. $NdCl_3$

The measurement of the heat capacity of $NdCl_3$ made it immediately apparent that the peaks observed in the magnetic susceptibility measurements could not be due to cooperative magnetic transitions involving all the ions in the crystal. Complete magnetic ordering within the ground-state doublet will result in an entropy change of $\Delta S=R\ln 2$. The total entropy change in $NdCl_3$ as calculated from the magnetic heat capacity over the entire region of the measurements, 0.3–4.0 K, is $\Delta S=0.545R=0.79R\ln 2$. The small amount of magnetic entropy above 4.0 K can be estimated by a T^{-2} extrapolation of the magnetic heat capacity. This leads to a value of the magnetic entropy at 0.3 K of $S_{mag}=0.137R=0.20R\ln 2$. Most of this observed entropy change, of course, is associated with the broad heat capacity anomaly and only 1 or 2% of it can be attributed to the peaks at 1.04 and 1.74 K. This leads one to suspect chemical impurities as the cause of the peaks. However, the shape of these anomalies in the heat capacity and susceptibility as well as the effect of an applied field on the heat capacity at 1.04 K indicate that they are probably cooperative ferromagnetic transitions, and therefore the ions involved cannot be dispersed uniformly throughout the crystal. One impurity likely to be present in aggregates is neodymium oxychloride, since it is insoluble in the trichloride melt. Susceptibility measurements on NdOCl, however, showed no peaks in the vicinity of those observed in $NdCl_3$. In any case we do not consider these peaks as a property of the pure material. We also ascribe the peak at 1.45 K in the heat capacity to impurity effects. This peak occurs in a temperature region where the susceptibility is varying smoothly and it is not affected by a magnetic field. As a result, we cannot be certain that it is of a magnetic origin. An antiferromagnetic transition, however, involving only a small fraction of the ions, could go undetected in the susceptibility and the transition would be little affected by an external field. In the following discussion we neglect the sharp peaks in the heat capacity and susceptibility in an attempt to determine the underlying magnetic behavior of this material.

The broad anomaly in the heat capacity of $NdCl_3$ is typical of the behavior predicted by linear chain models.[47,48] Such one-dimensional systems do not possess long-range order and the broad anomaly arises from the gradual increase in the extent of the short-range order. For long-range order to occur there must be some ordering influence other than that within the chains themselves. The thermal and magnetic properties of the linear Ising chain[47] are well known and can be calculated exactly. Recently, Bonner and Fisher[49] have developed a method of approximating the heat capacities and susceptibilities of linear chains in which the interactions between magnetic ions vary from pure Ising to pure Heisenberg. In Fig. 9 we compare the

[44] G. H. Wannier, Phys. Rev. **79**, 357 (1950).
[45] F. Varsanyi and J. P. Maita, Bull. Am. Phys. Soc. **10**, 609 (1965).
[46] B. Bleaney, Phys. Rev. **78**, 214 (1950).
[47] G. F. Newell and E. W. Montroll, Rev. Mod. Phys. **25**, 353 (1953).
[48] C. Domb, Advan. Phys. **9**, 149 (1960).
[49] J. C. Bonner and M. E. Fisher, Phys. Rev. **135**, A640 (1964).

heat capacity of the 3N's $NdCl_3$ sample (solid line) with curves calculated from antiferromagnetic linear chain models.[50] In these calculations the Hamiltonian, as used by Bonner and Fisher, is

$$\mathcal{H}=-2J\sum_{i=1}^{n}\{S_i^zS_{i+1}^z+\gamma(S_i^xS_{i+1}^x+S_i^yS_{i+1}^y)\}+\beta\sum_{i=1}^{n}\mathbf{H}_i\cdot\mathbf{g}\cdot\mathbf{S}_i, \quad (1)$$

which gives the Ising case with $\gamma=0$ and the Heisenberg case with $\gamma=1$. The dashed curves in Fig. 9 are linear Ising chain heat capacities given by

$$C/R=D^2\,\mathrm{sech}^2D, \quad (2)$$

where

$$D=J/2kT. \quad (3)$$

For the long-dashed curve, $J/k=-1.13$ K was chosen such that the heat capacity maximum of the calculated curve would occur at 0.47 K, the temperature of the experimental maximum. The dotted curve in Fig. 9 is obtained from Eq. (1) with $\gamma=0.5$ and $J/k=-0.72$ K. In the vicinity of the maximum the experimental curve is midway between the two calculated curves, whereas at higher temperatures the Ising curve gives a better fit. The heat capacity maxima at $\gamma=1$, 0.5, and 0 have C/R values of 0.350, 0.358, and 0.440, respectively, so the heat capacity near the maximum must be changing rapidly with γ at small values of γ. A value of γ intermediate to those used in Fig. 9 ($\gamma=0$ and 0.5) would improve the over-all fit.

In Fig. 10 the susceptibility of the 3N's $NdCl_3$ sample is compared with calculated susceptibilities, the upper set of curves representing measurements made with the measuring field perpendicular to the c axis and the lower set representing parallel measurements. The solid lines indicate the experimental measurements.[5] The dashed curves in both sets are for linear Ising chains and are given by[51,52]

$$\chi_\perp=A(\tanh D+D\,\mathrm{sech}^2D) \quad (4)$$

and

$$\chi_\parallel=Be^{2D}/T, \quad (5)$$

where D is given by Eq. (3), and A and B are arbitrary constants. The long-dashed curves have $J/k=-1.13$ K, the value used to fit the heat capacity maximum in Fig. 9. The short-dashed curves have $J/k=-1.32$ K, which gives an excellent fit to the perpendicular susceptibility over nearly the whole region but a rather poor fit to the heat capacity (see Fig. 9). The dotted parallel susceptibility curve is for $\gamma=0.5$. Although the large peaks in the experimental susceptibility make comparisons difficult, it does appear that the best fit to the parallel susceptibility would be for a γ somewhere between 0 and 0.5. Expressions for $\chi_\perp$ at intermediate γ values are not available, but since χ is isotropic for $\gamma=1$, we show this relation as the dotted perpendicular susceptibility curve in Fig. 10. To calculate this curve we used $J/k=-0.49$ K, the value which gives a heat capacity maximum at 0.47 K for $\gamma=1$. Again, it is apparent that an intermediate value of γ would give a reasonable fit to the experiment.

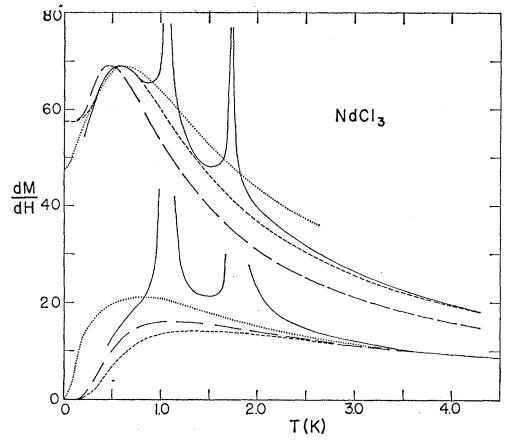

FIG. 10. Magnetic susceptibilities of $NdCl_3$. The upper set of curves is for the measuring field perpendicular to the c axis of the crystal and the lower set for the field parallel. The solid lines are the experimental curves for the 3N's sample. The dashed lines are linear Ising chain models with $J/k=-1.13$ and -1.32 K for the long and short dashes, respectively. The lower dotted curve is the linear chain model with intermediate anisotropy of $\gamma=0.5$ and $J/k=-0.72$ K. The upper dotted curve is the linear Heisenberg chain model with $J/k=-0.49$ K.

There are two other experimental measurements with which we can compare the J/k values used in the above curve fitting. Prinz[7] has measured the optical absorption spectrum of pure $NdCl_3$ and has interpreted the appearance of satellite lines on the basis of an Ising-type interaction between near-neighbor ions. These measurements yield a $J/k=-1.02$ K, in close agreement with our Ising model value. Brower, Stapleton, and Brower[25] and Baker, Riley, and Shore[26] have measured the interactions between pairs of Nd^{3+} ions in $LaCl_3$ using ESR techniques. This yields a quantity $a_{ij}-b_{ij}=-0.91$ K for nearest-neighbor interactions which can be converted to the terms used in the above expressions by

$$a_{ij}-b_{ij}=(2J/k)(1-\gamma).$$

For $\gamma=0.5$ this expression yields $J/k=-0.91$ K, a value somewhat larger than the $J/k=-0.72$ K obtained by fitting the heat capacity to the same γ. $\gamma=0$ yields $J/k=-0.45$ K, a value much smaller than that used for the Ising chain heat capacity. Again we find numerical results indicating a γ value between 0 and 0.5.

γ is related to the g values; those of dilute Nd^{3+} in $LaCl_3$ have been determined by ESR[8] to be $g_\parallel=3.996$ and $g_\perp=1.763$. From the optical spectra[7] the g values of 1% Nd^{3+} in $LaCl_3$ were measured to be $g_\parallel=4.00$ and $g_\perp=1.76$, and in pure $NdCl_3$ they were $g_\parallel=4.4$ and

[50] J. C. Bonner, thesis, University of London, 1968 (unpublished).
[51] J. S. Marsh, Phys. Rev. **145**, 251 (1968).
[52] S. Katsura, Phys. Rev. **127**, 1508 (1962).

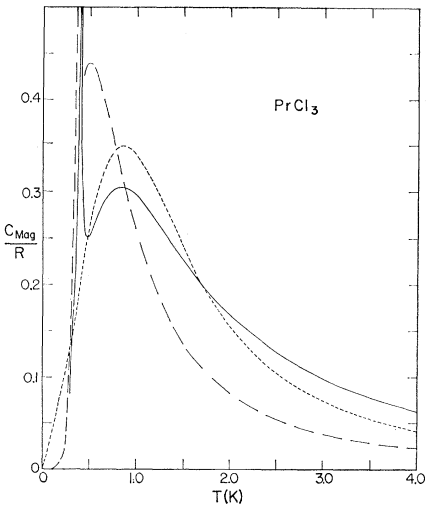

FIG. 11. Experimental and calculated heat capacity of $PrCl_3$. The solid curve represents the experimental results of the 5N's sample. The short-dashed curve is the calculated heat capacity based on the Heisenberg linear chain model [Eq. (1) with $\gamma=1$] with $J/k=-0.89$ K. The long-dashed curve is the calculated heat capacity using the model proposed by Stout and Chisholm with $J/k=-1.20$ K.

$g_\perp=1.56$. Using the latter values, one obtains[53]

$$\gamma=(g_\perp/g_{\parallel})^2=(1.56/4.4)^2=0.126,$$

which is in agreement with the above conclusions.

We must be careful not to carry these quantitative comparisons too far, since the results of the two samples measured indicate that the size of the sharp peaks influences the height of the heat capacity maximum. The entropy change, however, in the range 0.3–4 K is the same for the two samples. The larger entropy change in the 5N's sample near the 1.04-K peak is compensated by a smaller change in the region of the 0.47-K maximum.

Although these results indicate that $NdCl_3$ is behaving like a collection of independent linear chains, it does not rule out the possibility of long-range order occurring at some lower temperature. The NQR of the chlorine nuclei provides a sensitive probe of this and, in contrast to NMR, does not require an external magnetic field which would perturb the magnetic system. In general, long-range ordering causes the single NQR line to split into several components. The frequencies of the new resonance lines will be determined by the magnitude of the internal magnetic field and its direction with respect to the principal axes of the electric field gradient (EFG). In the present experiments an internal field of approximately 3×10^{-4} T is detectable. The gradual disappearance without broadening of the single resonance line and the eventual appearance of the fully split lines at lower temperatures is not the behavior typically observed with magnetic ordering. The observed splittings in $NdCl_3$, however, do indicate unambiguously the existence of a sublattice magnetization.

[53] In deriving this expression for γ we have assumed that the magnetic dipole and isotropic exchange interactions between the real spins are the dominant interactions.

The ^{35}Cl and ^{37}Cl NQR signals in $NdCl_3$ disappeared at 0.50 K, the temperature of the broad heat capacity maximum, and were not observable between 0.17 and 0.50 K. The three resonance lines observed below 0.17 K can be used to calculate the magnitude of the hyperfine field and its direction with respect to the principal axes of the EFG at the chlorine nucleus. The secular determinant corresponding to the nuclear-spin Hamiltonian

$$\mathcal{H}=\gamma_n\mathbf{B}\cdot\mathbf{I}+A'\{[3I_z^2-I(I+1)]+\tfrac{1}{2}\eta(I_+^2+I_-^2)\}$$

yields a fourth-degree polynomial. This was solved over a wide range in three parameters describing the magnitude and direction of the hyperfine field until the predicted transition frequencies agreed with experiment. The EFG asymmetry parameter, η, has not been determined for chlorine in $NdCl_3$ but was taken to be 0.58, the value[54] in $PrCl_3$. η is primarily determined by electrostatic interactions which should differ little for compounds of neighboring lanthanide ions. The average deviation of the fit using this value of η was 12 kHz. A line was predicted at 3.22 MHz but was not observed; its transition probability should be $\frac{1}{3}$ of that calculated for the 4.67- and 5.27-MHz lines. We should note that the calculated transition probabilities for the 4.67- and 5.27-MHz lines are approximately 1:1, whereas the experimentally observed ratio is 1:10. The calculated parameters were $B=0.252$ T, $\theta=0.80\pm0.02$ rad ($46°\pm1°$), and $\phi=0.35\pm0.03$ rad ($20°\pm2°$), where θ and ϕ are the polar and azimuthal angles, respectively. These values can now be used to predict the resonance frequencies of the ^{37}Cl nuclei. The two most intense lines were predicted to occur at 3.74 and 4.30 MHz; weak resonances were observed at 3.82 and 4.26 MHz, thus confirming the model. On the basis of the NQR results we predict a heat capacity anomaly due to long-range ordering, in the temperature range 0.17–0.30 K.

B. $PrCl_3$

The heat capacity of $PrCl_3$ as shown in Fig. 3 has the broad anomaly of the linear chain models with the maximum occurring at 0.85 K. Here, however, it is accompanied by a peak at 0.4 K, which is indicative of long-range ordering. That it is, in fact, associated with long-range order is confirmed by the observation of the splitting of the NQR line at 0.428 K, which indicates the onset of a spontaneous sublattice magnetization. The susceptibility shown in Fig. 3 is similar to that of the antiferromagnetic linear chain models. It shows no effect due to the long-range ordering at 0.4 K, but with the susceptibility already decreasing rapidly toward zero at that temperature, any change in its rate of decrease would be hard to detect.

Behavior of this type is well known, at least from a theoretical viewpoint. In a classic paper on solutions of the rectangular Ising net problem, Onsager[55] solved an example where the interactions in one direction were

[54] W. E. Hughes, C. G. Montgomery, W. G. Moulton, and E. H. Carlson, J. Chem. Phys. **41**, 3470 (1964).

[55] L. Onsager, Phys. Rev. **65**, 117 (1944).

100 times greater than those in the other direction. The heat capacity of this model shows a close similarity to the observed heat capacity of $PrCl_3$. The behavior of the rectangular Ising net model is identical with that of the linear Ising chain model down very close to the temperature at which long-range order occurs. By analogy, we might expect the heat capacity of $PrCl_3$ in the temperature region of the broad anomaly and above to approximate that of the linear chain models as was found with $NdCl_3$. Unfortunately, we find that a good fit to the experimental data cannot be obtained for any value of γ. Varying γ from 0 to 1 decreases the value of the heat capacity maximum from $0.44R$ to $0.35R$ but the maximum of the broad anomaly in the 5N's $PrCl_3$ sample is only $0.31R$ ($0.29R$ for the 3N's sample). Calculated values of the heat capacity and susceptibility for $\gamma=1$ and $J/k=-0.89$ K are shown as the short-dashed curves in Figs. 11 and 12, respectively; the solid curves represent the experimental values of the 5N's sample. The interaction constant was chosen such that the calculated and experimental heat capacity maxima occur at the same temperature. Note that this results in the calculated susceptibility maximum occurring at nearly the same temperature (1.13 K) as the experimental maximum (1.05 K). For the Ising model with J/k chosen by the same criterion, the calculated susceptibility maximum would occur at nearly twice that temperature (2.04 K). The nonzero intercept of the calculated susceptibility in Fig. 12 is unrealistic; it results from the isotropic nature of the Heisenberg model and even a vanishingly small anisotropy will cause this intercept to go to zero. Although the Heisenberg model gives the best fit of all the linear chain models to the short-range-order portion of the experimental results, it cannot be correct since the measured g values[8] in $PrCl_3$ are very anisotropic: $g_{\parallel}=1.035$ and $g_{\perp}=0.1$.

In considering interchain interactions we make some use of Onsager's two-dimensional model but for the most part we use the more appropriate three-dimensional model of Stout and Chisholm.[56] Both of these models use the critical temperature T_c (the Néel point) as a known parameter. This quantity is somewhat ambiguous in the present case. The NQR splitting gives $T_c=0.428$ K. At this temperature[57] the heat capacity is just beginning to increase again with decreasing temperature, and the heat capacity maximum is at 0.41 K. We use the value 0.428 K, since the onset of long-range order as indicated by the spontaneous magnetization is the more fundamental definition of T_c.

The treatment of Stout and Chisholm is based on linear Ising chains coupled by a molecular field. This theory has one adjustable parameter, the intrachain interaction constant J/k. Since the Ising chain model is a poor approximation to the experimental results, it is

[56] J. W. Stout and R. C. Chisholm, J. Chem. Phys. **36**, 979 (1962).

[57] These temperatures were measured on different temperature scales, but a careful evaluation of their accuracy indicates that the two scales do not differ by more than 5 mK at 0.4 K.

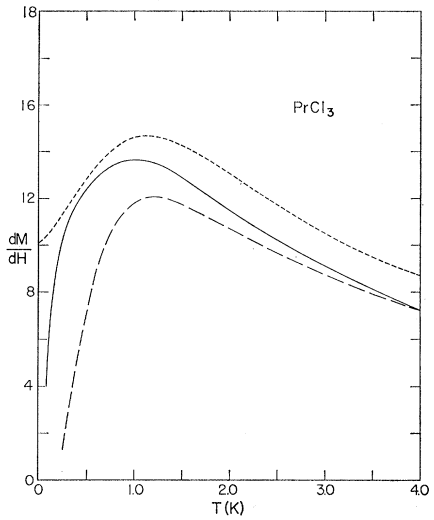

FIG. 12. Measured and calculated magnetic susceptibility of $PrCl_3$. The solid curve represents the experimental results of the 5N's sample. The short-dashed curve is the susceptibility calculated using the Heisenberg linear chain model [Eq. (1) with $\gamma=1$] with $J/k=-0.89$ K. The long-dashed curve is the susceptibility calculated using the model of Stout and Chisholm with $J/k=-1.20$ K. The ordinate is the differential magnetic susceptibility in arbitrary units.

difficult to decide on a value of J/k. We use a mehodt suggested by Stout and Chisholm of equating the entropies of the model and the experiment at T_c. This gives $J/k=-1.20$ K ($S_{\mathrm{mag}}=0.177R$ at 0.428 K). The heat capacity and magnetic susceptibility calculated by this model are shown as the long-dashed curves in Figs. 11 and 12. The susceptibility was calculated using Eq. (5). In the expression given by Stout and Chisholm,[56]

$$\chi=Be^{2D}/(T+T_ce^{2(D+D_c)}),$$

where $D_c=J/2kT_c=-1.40$, the term $T_ce^{2(D+D_c)}$ makes a negligible contribution over the range of the measurements and, hence, has been neglected.

The shift of the nuclear resonance line in the magnetically ordered state from the NQR frequency in the paramagnetic state is proportional to the sublattice magnetization. In Fig. 13 we have compared the experimentally observed variation with temperature with three theoretical models. The solid curve is calculated by the theory of Stout and Chisholm using the parameters given above. The short-dashed curve is the Weiss molecular-field model with a spin $S=\frac{1}{2}$. The spontaneous magnetization for a rectangular Ising net is given by[58,59]

$$[M(T)/M(0)]^8=1-16x^2y^2[(1-x^2)^2(1-y^2)^2]^{-1},$$

where $x=e^{J_1/kT}$ and $y=e^{J_2/kT}$. J_1/k is determined by the position of the broad maximum in the heat capacity curve and was taken to be $J_1/k=-2.04$ K. J_2/k can be calculated from the requirement that

$$\sinh(J_1/kT)\sinh(J_2/kT)=1$$

[58] R. B. Potts, Phys. Rev. **88**, 253 (1952).

[59] C. H. Chang, Phys. Rev. **88**, 1422 (1952).

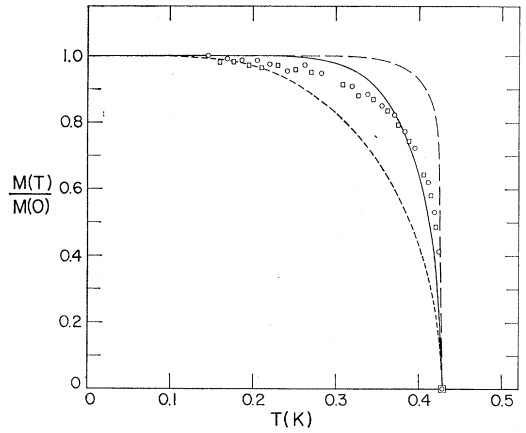

FIG. 13. Experimental and calculated sublattice magnetization of $PrCl_3$. The circles represent the higher-frequency branch and the squares represent the lower-frequency branch of the data in Fig. 4. The short-dashed curve is the magnetization based on the molecular field for $S=\frac{1}{2}$. The long-dashed curve is the magnetization calculated by using the rectangular Ising net model with $J_1/k=-2.04$ K and $J_2/k=-7.4\times10^{-3}$ K. The solid curve is the magnetization calculated by using the model of Stout and Chisholm with $J/k=-1.20$ K. The ordinate is the ratio of the magnetization at any given temperature T and the magnetization at $T=0$ K.

at the critical point.[55] If the critical temperature is taken as 0.428 K, then $J_2/k=-7.4\times10^{-3}$ K. The magnetization of the rectangular Ising net calculated using these values is shown as the long-dashed curve in Fig. 13. It can be seen that the model of Stout and Chisholm, as expected, is in better agreement with experiment than the other two models.

The observation of only two resonance lines in the ordered state would imply that an effective magnetic field of 1.06×10^{-2} T at the chlorine site is parallel to the principal axis of the EFG, since any other direction will result in a four-line spectrum. Measurements by Hessler and Carlson[38] indicate that $\theta=68°$ and $\phi=22°$, where θ and ϕ are the polar and azimuthal angles, respectively. We are, however, unable to fit our observed lines using these values in the Hamiltonian. A four-line spectrum is also predicted if the magnetic field has the same orientation as that in $NdCl_3$. In that case the missing resonances should be at 4.757 and 4.385 MHz with intensities approximately one-third that of the observed lines, and the magnitude of the field would be $(2.70\pm0.10)\times10^{-2}$ T.

The loss of intensity without observable broadening of the NQR lines in $NdCl_3$ and $CeCl_3$ is to be contrasted with the observation of a nuclear resonance signal at all temperatures in $PrCl_3$. Abragam[60] has discussed the effect on a nuclear resonance line of the fluctuations of neighboring electronic moments. In a paramagnet the exchange coupling J between magnetic ions induces flip-flops between neighboring electron spins at a frequency of the order of J/h. The condition that the average electronic field will be effective in a nuclear resonance experiment is that $A\tau\ll1$, where A is the hyperfine coupling constant and $\tau\sim h/J$. The linewidth contribution will be of the order of $A^2\tau$. The electronic field, furthermore, will be averaged until the flip rate is comparable with the nuclear resonance linewidth. In the present experiments this is approximately 10^4 sec^{-1}. The absence of any observable resonance in the temperature range $0.17<T<0.50$ K in $NdCl_3$ indicates that a magnetic field at the chlorine nuclei makes a contribution to the linewidth, i.e., $A^2\tau\gg10^4$ Hz. Also, the condition $A\tau\ll1$ is not satisfied. This is consistent with the heat capacity measurements which indicate extensive short-range order in this temperature region. We conclude that in $NdCl_3$ "short-range order" means that the magnetic environment at any one lattice site changes in a time longer than 10^{-6} sec $(1/A)$ but less than the time required to sweep through a resonance, i.e., a few seconds. This also applies qualitatively to $CeCl_3$ in the temperature range 0.054–0.110 K. In $PrCl_3$ the characteristic time τ is less than $1/A$, i.e., 10^{-5} sec, since the resonance is observed throughout the short-range-ordering region.

Some of the observed differences between the two $PrCl_3$ samples are worthy of comment. The magnetic entropy changes calculated[61] from the heat capacity measurements for the temperature range 0.3–4.0 K are $\Delta S_{\rm mag}=0.536R=0.775R\ \ln2$ for the 3N's sample and $\Delta S_{\rm mag}=0.577R=0.833R\ \ln2$ for the 5N's sample. Using a T^{-2} extrapolation of the magnetic heat capacities above 4.0 K, the magnetic entropies at 0.3 K can be determined; these are $S_{\rm mag}=0.121R=0.175R\ \ln2$ for the 3N's sample and $S_{\rm mag}=0.084R=0.121R\ \ln2$ for the 5N's sample. With approximately 40% more entropy remaining in the 3N's sample than in the 5N's sample at 0.3 K, the heat capacity of the 3N's sample below that temperature must be significantly greater than that of the 5N's sample if the full $R\ \ln2$ entropy change is to be realized for both samples.

C. $CeCl_3$

In the heat capacity of $CeCl_3$ shown in Fig. 5 there is a small but pronounced peak at 1.0 K. This peak occurs in a temperature region where the susceptibility is varying smoothly and it is not affected by a magnetic field. In this respect it is related to peaks observed for each of the samples measured except $PrCl_3$. We have already attributed the similar peak appearing at 1.45 K in the heat capacity of $NdCl_3$ to impurity effects but for this peak in $CeCl_3$ we have convincing evidence. Keen *et al.*[6] observed a similar peak at the same temperature in their $CeCl_3$ heat capacity measurements but found it was absent in measurements made on selected "optically clear" crystals. Also, their susceptibility measurements did not have a peak at 0.345 K as we observed. We believe that this peak is due to the same

[60] A. Abragam, *The Principles of Nuclear Magnetism* (Oxford University Press, London, 1961), p. 195.

[61] The correction used for the nuclear heat capacity is for paramagnetic materials and will not be strictly correct in the long-range-order region. The calculated nuclear entropy which has been subtracted from the experimental entropy to obtain the magnetic entropy is $\Delta S/R=0.021$ above 0.3 K.

kind of aggregation of ferromagnetic chemical impurities as those producing the two sharp peaks in $NdCl_3$.

Keen *et al.*[6] have made measurements down to 0.26 K and find that the heat capacity exhibits a maximum of $C>3R$ at 0.27 K. (See note added in proof.) We have fitted a linear Ising chain model to our data at 0.3 K (which defines J/k as -0.31 K) and find that it fits the data very well from 0.29 K, the lowest temperature of the measurements, to 0.55 K. The short-dashed curve in Fig. 5 shows this calculated curve through the region of the impurity peak.[62] Keen *et al.*[6] report the magnetic heat capacity above 0.7 K to vary as $C/R=0.0185T^{-2}$, whereas the linear Ising model with $J/k=-0.31$ K gives $C/R=0.024T^{-2}$ at high temperatures. The heat capacity of this Ising model has its maximum at 0.13 K, approximately the temperature at which the NQR signal disappears.

We have measured the ^{35}Cl NQR spectra as a function of temperature in order to determine the $CeCl_3$ transition temperature and the sublattice magnetization. As stated in Sec. 3 C, there was no splitting in the NQR line and the intensity of the NQR signal varied inversely with temperature at temperatures higher than 0.20 K. In particular, there was no change in the NQR signal in the vicinity of 0.27 K, where a peak in the heat capacity has been reported.[6] We conclude that any magnetic field at the ^{35}Cl nucleus averages to zero in a time of the order of the resonance linewidth. Hence the heat capacity peak at 0.27 K cannot be associated with long-range magnetic ordering. Calculations show that any static arrangement of the Ce spins will result in a dipolar magnetic field at the Cl site. It follows that if the magnetic field is zero, then the transferred hyperfine field must be equal and opposite to the dipolar field; an unbalance of 3×10^{-4} T would be detectable.

The reduction in signal intensity, without observable broadening, in the temperature range 0.11–0.20 K is similar to the behavior in $NdCl_3$ in the short-range-ordering region. By analogy with $NdCl_3$ one would expect an anomaly, associated with short-range order, in the heat capacity with a maximum at approximately 0.11 K. One would also expect the heat capacity to have a peak at some lower temperature due to the onset of long-range order.

D. $SmCl_3$

In Fig. 6 the heat capacity data are shown by the open circles through which a solid line has been drawn. There is a sharp, λ-shaped peak at 1.1 K which we attribute to the same kind of impurities that produce similar peaks in $CeCl_3$, $CeBr_3$, and $NdCl_3$ at 1.0, 1.4, and 1.45 K, respectively. These peaks have been discussed in connection with the $CeCl_3$ heat capacity data. Unlike the other rare-earth trihalide heat capacity data presented here, the $SmCl_3$ magnetic heat capacity is increasing with increasing temperature at 4.0 K. If the first excited energy level were lower by 20% in the concentrated salt than that reported for the dilute salt, then the low-temperature tail of the associated Schottky anomaly would account for the shape of the curve.

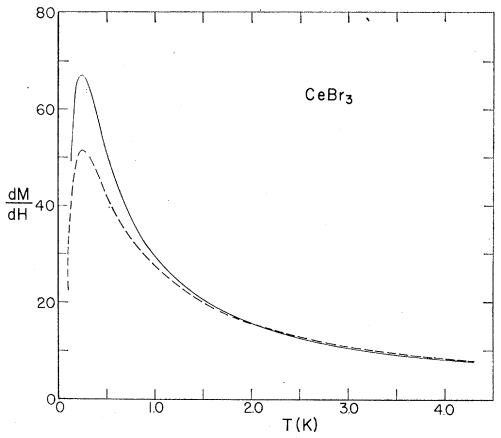

FIG. 14. Experimental and calculated differential magnetic susceptibility of $CeBr_3$. The solid curve represents the experimental results. The dashed curve is the susceptibility calculated by using the linear Ising chain model with $J/k=-0.25$ K. The ordinate is the differential magnetic susceptibility in arbitrary units.

Since $g_{\parallel}$ and $g_{\perp}$ for Sm^{3+} in $LaCl_3$ are very nearly the same, one would expect that the magnetic properties of $SmCl_3$ could be described quite well by the antiferromagnetic linear Heisenberg chain model [Eq. (1) with $\gamma=1$]. Indeed, we find that the susceptibility is fitted quite accurately by this model with $J/k=-0.27$ K. The heat capacity calculated with this model, however, does not fit the experimental data at all. The calculated curve is increasing rapidly with decreasing temperature in the vicinity of 0.5 K.

Unlike the ^{35}Cl NQR signal in $CeCl_3$, $PrCl_3$, and $NdCl_3$, the linewidth of the ^{35}Cl NQR signal in $SmCl_3$ did broaden somewhat between 0.32 and 0.21 K, at which latter temperature the signal disappeared. The disappearance of the signal, however, was not due primarily to broadening but, we believe, due to the same reasons that the signals in $CeCl_3$ and $NdCl_3$ disappeared. There was no change in the NQR signal in the vicinity of the heat capacity peak at 1.1 K.

E. $CeBr_3$

The susceptibility of $CeBr_3$ with a maximum at 0.25 K is not at all similar to the susceptibility of $CeCl_3$, which has a sharp peak at 0.35 K. The peak in the $CeBr_3$ results is qualitatively very similar to that calculated for an antiferromagnetic linear Ising chain model as shown in Fig. 14. Quantitatively, however, the fit of the antiferromagnetic linear Ising chain model to the data is not very good. The dashed curve in Fig. 14 was calculated from the expression $\chi=Be^{2D}/T$, where $D=J/2kT$ and $J/k=-0.25$ K. J/k was chosen such

[62] The entropy associated with the heat capacity difference between the calculated and measured curves is $\Delta S=0.0115R=0.017R\ln 2$, implying that only 1.7% of the Ce^{3+} ions are involved in the impurity peak.

that χ would have a maximum value at 0.25 K. The ordinate scale is arbitrary and the calculated curve was forced to fit the data at 2.50 K.

The magnetic susceptibility shows no evidence of a transition of any kind at the position of the peak in the heat capacity at 1.4 K. We believe that this peak is due to the same kind of chemical impurities that produce the peaks at 1.0 K in $CeCl_3$, 1.1 K in $SmCl_3$, and 1.45 K in $NdCl_3$. If one ignores this peak and fits the heat capacity at temperatures below 0.7 K to Eq. (2), then $J/k=-0.39$ K. The dashed curve in Fig. 7 is this calculated curve.[63] It should be noted that this value of J/k is considerably different from that used to fit the susceptibility results. We have no explanation for this discrepancy.

5. SUMMARY

In the heat capacity of nearly all the samples measured there are small anomalous peaks, several of which are accompanied by large spikes in the susceptibility measurements. We have concluded that these anomalies are due to impurity effects and we have ignored them in order to analyze what is believed to be the magnetic properties of the pure materials.

The magnetic susceptibility and heat capacity measurements have shown that there is extensive short-range order in all of the compounds, $CeCl_3$, $PrCl_3$, $NdCl_3$, $SmCl_3$, and $CeBr_3$. This is indicated in the heat capacity of $PrCl_3$ and $NdCl_3$ by a broad anomaly, in which approximately 80% of the total magnetic entropy change of $R\ln 2$ occurs. For the other compounds we were able to study only the high-temperature part of the anomaly, since the lowest temperature of the heat capacity measurements was ~ 0.3 K. Furthermore, on the low-temperature side of the heat capacity anomaly in $PrCl_3$ we found a sharp peak at 0.41 K, indicating the onset of long-range order. This was confirmed by Cl NQR measurements. The NQR line split into two components at 0.428 K, and from the magnitude of the splitting we have found an effective internal field at the Cl nucleus of 1.06×10^{-2} T and its direction is parallel to that of the principal axis of the EFG. The heat capacity of $NdCl_3$ did not have a peak indicating the onset of long-range order in the temperature region of our measurements, but the NQR results show that for $T\leq 0.17$ K there is indeed long-range order and that the sublattice magnetization has essentially already reached its maximum value at 0.17 K, the temperature at which the new NQR lines appear. No NQR signals were observed between 0.17 and 0.50 K. On this basis, we predict that there is a peak, indicating the onset of long-range order, in the heat capacity between 0.17 and 0.30 K. The field at the Cl nucleus in $NdCl_3$ is 0.252 T and its direction, relative to the principal axes of the EFG, is defined by a polar angle of 0.80 ± 0.02 rad ($46°\pm 1°$) and an azimuthal angle of 0.35 ± 0.03 rad ($20°\pm 2°$).

The Cl NQR signal in $CeCl_3$ disappeared at 0.110 K, and we were unable to observe any resonances between 0.054 K, the lowest temperature of our measurements, and 0.110 K. By analogy with $NdCl_3$, we interpret this to mean that there is an anomaly, associated with short-range order, in the heat capacity with a maximum near 0.110 K, with long-range order appearing at some lower temperature. The heat capacity results above 0.29 K are consistent with this conjecture.

The heat capacity and susceptibility results of $SmCl_3$ indicate a wide region of short-range ordering. The Cl NQR signal disappeared at 0.21 K, in a manner similar to that in $NdCl_3$ and $CeCl_3$, and we were unable to observe any resonances between 0.13 and 0.21 K.

The heat capacity and magnetic susceptibility of $CeBr_3$ are behaving in a manner very similar to that observed in $CeCl_3$ but indicate that magnetic ordering will probably occur at a higher temperature in the bromide than in the chloride.

6. CONCLUSION

From the combination of magnetic susceptibility, heat capacity, and NQR results we conclude that the dominant interactions in $CeCl_3$, $PrCl_3$, $NdCl_3$, $SmCl_3$, and $CeBr_3$ are antiferromagnetic nearest-neighbor interactions in agreement with the analyses of pair spectra.[24–27] These give rise to antiferromagnetic linear chains with only small interactions between the chains. The small interchain interactions ultimately cause a three-dimensional antiferromagnetic long-range ordering with the concomitant sublattice magnetization. The magnetically ordered structures of these materials is not completely determined and it would be fruitful to do neutron diffraction studies of them below their Néel temperatures in order to determine the magnetic structures. Measurements on better-quality crystals would be desirable to clear up the ambiguity about the peaks which we have attributed to impurity effects.

Note added in proof. W. P. Wolf and D. P. Landau have informed us that the peak at 0.27 K is spurious. They have remeasured the heat capacity down to 0.060 K and find a broad maximum at approximately 0.15 K and a sharp peak, indicating long-range order, at 0.105 K.

ACKNOWLEDGMENTS

We are indebted to Dr. R. J. Soulen for his assistance and for the use of his ^{3}He-^{4}He dilution refrigerator in the NQR experiments on $CeCl_3$. We gratefully acknowledge the interest which has been shown by Dr. R. P. Hudson in the work reported here. Also, we would like to thank Dr. J. C. Bonner for a copy of her thesis.

[63] The difference in the entropy changes derived from the calculated and measured heat capacities between 0.7 and 4.0 K is $\Delta S=0.025R=0.036R\ln 2$.